Energy xxx (xxxx) xxx

Contents lists available at ScienceDirect

Energy

journal homepage: www.elsevier.com/locate/energy

Mathematical modelling of gasification process of sewage sludge in reactor of negative CO_2 emission power plant

Paweł Ziółkowski [a, *], Janusz Badur [b], Halina Pawlak- Kruczek [c], Kamil Stasiak [a], Milad Amiri [a], Lukasz Niedzwiecki [c], Krystian Krochmalny [c], Jakub Mularski [c], Paweł Madejski [d], Dariusz Mikielewicz [a]

[a] Gdańsk University of Technology, Faculty of Mechanical Engineering and Ship Technology, Institute of Energy, Gdańsk, Poland
[b] Energy Conversion Department, Institute of Fluid Flow Machinery, Polish Academy of Sciences, Gdańsk, Poland
[c] Wrocław University of Science and Technology, Faculty of Mechanical and Power Engineering, Department of Energy Conversion Engineering, Wrocław, Poland
[d] AGH University of Science and Technology, Department of Power Systems and Environmental Protection Facilities, Faculty of Mechanical Engineering, Poland

ARTICLE INFO

Article history:
Received 20 July 2021
Received in revised form
26 October 2021
Accepted 9 November 2021
Available online xxx

Keywords:
CCS
Sewage sludge
Gasification
CO2 negative power plant
Thermodynamic equilibrium

ABSTRACT

Sewage sludge is a residue of wastewater processing that is biologically active and consists of water, organic matter, including dead and alive pathogens, as well as organic and inorganic contaminants such as polycyclic aromatic hydrocarbons (PAHs) and heavy metals. Due to the nature of sewage sludge and its possible influence on human health and wellbeing, it is a subject of various regulations. Currently, sewage sludge is considered as biomass, according to the new Polish act on renewable energy sources of February 20, 2015 and its novel version of July 19, 2019. This study presents a novel model, along with a comparison with experimental results. The model could be used for sewage sludge gasification modelling for accurate assessment of the performance of novel concepts bioenergy with carbon capture and storage (BECCS) installations, using sewage sludge as a fuel. The composition of the dry produced gas, determined experimentally, yields: $X_{CO} = 0.093$, $X_{CO2} = 0.264$, $X_{CH4} = 0.139$, $X_{CxHy} = 0.035$, and $X_{H2} = 0.468$. Performed modifications to the original Deringer-with-Gumz-modification gasification model allowed to obtain good agreement with the experimental results, reaching $X_{CO} = 0.071$, $X_{CO2} = 0.243$, $X_{CH4} = 0.139$, $X_{C3H8} = 0.035$, and $X_{H2} = 0.512$. The main novelty in the formulas of the internal model was due to propane inclusion, which was not found in the literature before. Additionally, sulphur dioxide was applied in exchange for other sulphur components presented in the original model. Equilibrium constants were adjusted to suit the experimental model. For ease of calculation, the own code was used to iterate multiple temperatures. Included was the energy balance equation that is essential for verification.

1. Introduction

One of the challenges, for mankind, in the upcoming decades will be the joint effort in decreasing emissions of greenhouse gases (GHG) in order to comply with the Paris Agreement, signed in multilaterally by the majority of the countries all over the world [1]. Achieving such an ambitious goal requires a difficult transition towards decarbonisation and an increased share of renewables in the energy mix [2,3]. One of the established routes towards decarbonisation is the use of biomass, which is an important renewable energy source with significant potential in Europe [4]. Biomass can come from various sources, such as forestry [5–8], agriculture [9–13], or different types of waste streams [14–17], including sewage sludge [18,19]. Sewage sludge is a biologically active residue of the wastewater processing, containing water and organic matter, including pathogens, organic and inorganic contaminants, e.g. polycyclic aromatic hydrocarbons (PAHs) and heavy metals [19–21]. Utilization methods, allowing stabilization and safe recycling, gradually replace storage, landfilling and land spreading due to increased environmental restrictions (e.g. odour related regulations or EU Nitrate Directive) [22]. Thermal routes of sewage sludge utilization are currently a subject of active investigation due to increasingly common restrictions on landfilling

* Corresponding author.
E-mail addresses: pawel.ziolkowski1@pg.edu.pl (P. Ziółkowski), kamil.stasiak@pg.edu.pl (K. Stasiak).

https://doi.org/10.1016/j.energy.2021.122601

[18]. Among thermal methods, incineration is well established, mostly applying fluidized bed and grate furnaces [23,24]. Among novel utilization routes, processes such as mechanical disintegration [25–27], torrefaction [28–31], hydrothermal carbonization [32–34], or pyrolysis [35]. Another way to decrease global CO_2 emissions is Carbon Capture and Storage (CCS), which is a recognized mitigation technology within the UNFCCC and potentially can play an important role in mitigating anthropogenic emissions of CO_2 [36]. Much work is still needed, regarding the development of novel CCS technologies, taking into account efficiency, cost and water footprint [37]. Novel solutions are currently being developed, including carbon sequestration using hydrates [38–41], membrane-based carbon capture and storage [42,43] as well as pre-combustion CO_2 capture [44]. Most of the work has been done so far on post-combustion CCS. In this case, proper integration of CCS with power plants is crucial [45,46], taking into account the grid as well [47]. For post-combustion CO_2 capture, the biggest challenge is the dilution of CO_2 among the flue gases, which was the main driving factor for works on combustion with different levels of oxygen dilution [48,49]. Concepts based on oxy-combustion have been proven for natural gas [50], with suitability for retro fitting in a GTCC CHP [51]. Furthermore, adding sewage sludge gasification allows synergetic benefits in such cycles, by turning them into bioenergy with carbon capture and storage installation (BECCS). Recently such benefits have been proven for such a cycle, using gasification of sewage sludge [52]. Gasification is a process converting solid fuel into combustible gas, suitable for various materials of biological origin, including sewage sludge [53–56]. Gasification of sewage sludge has been investigated for various types of gasifiers and process conditions [57,58]. The possibility to use producer gas, from sewage sludge gasification, in a spark-ignition engine has been proven [59]. However, the addition of 40% of CH_4 to the producer gas from sewage sludge, is needed for satisfactory performance of a spark-ignition engine [60]. Laminar flame speed increases with increasing hydrogen content, which makes significant difference in terms of combustion of the gas [61]. Relatively high hydrogen content, reaching 30%–40% has been reported for sewage sludge gasification in fixed bed and fluidized bed gasifiers [62,63]. However, relatively low temperature of gasification for sewage sludge, may lead to high concentrations of tars, mainly phenols and their derivatives [19]. It has been demonstrated that reduction of tar content in producer gas could be achieved using plasma [64]. Therefore, plasma gasification has been a source of increased interest in the research community, as such gasification system can provide relatively high temperatures [65]. Using producer gas from sewage sludge in BECCS units requires use of gasification agents not containing inert gases, in order to facilitate CO_2 capture. Steam could be used for this purpose. However, suitable models are needed in order to produce reliable results of the composition of producer gas from steam gasification, which could be used as an input data for further optimisation of such BECCS installations. The aim of this paper is calibration of the Deringer-Gumz-modification model in order to give more accurate results for steam gasification of sewage sludge. Such calibration, based on experiments, can be implemented in practice by correction of rate coefficients and inclusion of additional reaction, that leads to creation of propane. Uncorrected model tends to overestimate CO production, which could lead to significant differences in terms of calculated and measured composition, especially at lower temperatures of gasification.

2. Materials and methods

2.1. Experimental setup

Gasification tests were performed using a laboratory-scale allothermal batch gasifier (Fig. 1), heated by a mantle made of 3 band heaters, installed on the sidewalls of the reactor. The temperature of the reactor was controlled by a PLC controller, with a K type thermocouple installed inside of the ceramic refractory of one of the band heaters. The temperature of the mantle was set to 900 °C for all the tests, which resulted in an average bed temperature of approximately 760 °C. The temperature was measured using a 1st class K type thermocouple and a digital thermometer. A sample of 1000 g was placed on a heat resistant steel mesh inside of a closed, hot reactor. It was anticipated that the layer of the material would resemble a layer on a grate in case of a subsequent scaling up of the gasifier. This was expected to give some indication of the feasibility of the use of a travelling grate in the conceptual gasifier. Gasification, in all of the cases, was performed using steam as a gasifying agent. Steam was fed directly under the bottom mesh (grate) of the sample basket. For both tests, the steam generator was set in a way allowing the constant generation of 1000 g of live steam per hour, with an outlet temperature of 96 °C.

A sample of the produced gas was taken from the top of the reactor and went through a series of impinger bottles filled with isopropanol. The first impinger bottle was installed, using a laboratory grip, in the vicinity of the gas outlet, in order to minimize the length of the PTFE hose, connecting the gas outlet of the gasifier with the aforementioned impinger bottle (Fig. 1). A series of three impinger bottles, connected to the outlet of the first impinger, was immersed in a PLC controlled cooling bath SD 07R-20. The bath was filled with ethylene glycol, and the temperature was set to be −15 °C. After leaving the series of impinger bottles, dry, cold gas went through the conditioner, with a built-in pump that helped to overcome the pressure drop introduced by the series of impingers. This allowed sampling of the gas with a sufficiently high volumetric flow rate (at least 1.0 l/min required by the analyzer). The composition of permanent gases in dry producer gas was determined online using a Gas 3100R analyzer. This analyzer uses NDIR (Non-Dispersive Infra-Red) sensors for measurements of CO_2, CO, CH_4 and C_xH_y (light hydrocarbons, given as an equivalent of methane). A TCD (Thermal Conductivity Detector) sensor is used to measure the H_2 content, whereas an electrochemical sensor is used for the determination of the O_2 content. The analyzer was calibrated using nitrogen of the purity of 5.0 before each measurement. The maximum permissible error, according to the data provided by the supplier of the Gas 3100P analyzer (Atut Sp. Z o. o., Lublin, Poland), is 2% of the measuring range for NDIR sensors for CO_2, CO, CH_4, C_xH_y, measuring range in the case of the TCD sensor for H_2, as well as an electrochemical sensor for O_2. The measuring ranges were as follows: CO_2, 40%; CO, 40%; CH_4, 10%; C_xH_y, 5%; H_2, 55%; and 25% in the case of O_2. Gas 3100R has a linearity drift of 1% of measuring range per week, both for zero and for span. The uncertainty (with p = 95%) was calculated according to the following equation:

$$U = k \cdot \frac{MPE}{\sqrt{3}} \tag{1}$$

where:

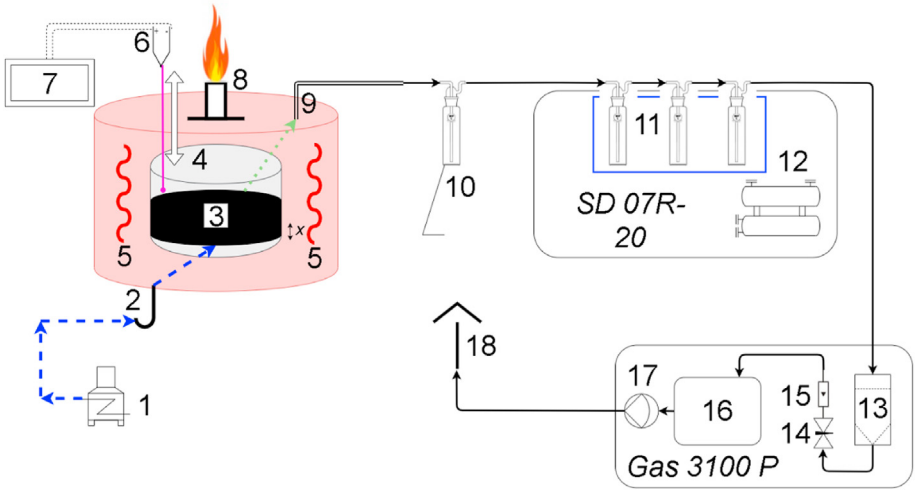

Fig. 1. Allothermal gasifier – diagram of the test rig (1 – steam generator; 2 – steam injection point; 3 – fixed bed of sewage sludge; 4 – heat-resistant steel mesh basket; 5 – band heaters; 6 – K type thermocouple; 7 – digital thermometer; 8 – flare; 9 – producer gas sampling point; 10 – Dreschl type impinger bottle, filled with isopropanol; 11 – cooling bath with Dreschl type impinger bottles, filled with isopropanol, immersed in ethylene glycol; 12 – glycol cooler; 13 – filter; 14 – needle valve for regulation of the gas flow through analyzer; 15 – rotameter; 16 – gas analyzer detectors and measuring cells; 17 – pump; 18 – vent).

U – uncertainty of measurement of a gas compound,
k – coverage factor (assumed to be 2).
MPE – maximum permissible error for the compound present in the gas.

The moisture content of the solid fuel sample was determined using the moisture analyzer Radwag MA. X2.A, with a scale resolution of 0.001 g and a maximum sample mass of 50 g. The program of the moisture analyzer was set to increase the temperature to 105 °C and then maintain it until the equilibrium mass of the sample was achieved. The mass of the sample was considered to be in equilibrium when the first derivative of the mass (dm/dt) was equal to or smaller than 1 mg/min. Volatile matter of all the dried samples was performed using TGA/DTG Pyris Diamond from PerkinElmer by heating the sample in a nitrogen of 99.99% purity up to 900 °C with a heating rate of 200 °C/min and a hold period of 20 min. Ash content was determined, using the gravimetric method, with ashing performed at 815 °C. The ultimate analysis was performed using a PerkinElmer 2400 analyzer, according to the procedure set in the standard EN ISO 16948:2015. HHV of both feedstock and product was determined, according to the procedure from EN 14918:2009, using IKA C2000 calorimeter. LHV (Lower Heating Value) was calculated, based on HHV (Higher Heating Value), moisture content after mechanical dewatering and hydrogen content of the fuel, using the appropriate formula from EN 14918:2009.

Table 1 presents gasification process data. The converter is steam with no air.

After mechanical dewatering of sewage sludge and before feeding it to the gasifier, it was additionally pre-dried to further reduce the moisture content without impacting the organic composition. Drying occurred at the temperature of 80 °C, which ensured that the bacterial population of, e.g., E. Coli or Legionella would decline [66,67]. Similarly to Akkache et al. [63], after drying at about 80 °C, the pre-dried sewage sludge with assumed 2% moisture content was introduced in the gasifier reactor at the temperature of 70 °C.

Table 2 shows the sewage sludge data that was used in the experiment, with mass fractions of elements like Carbon (C), Hydrogen (H), Nitrogen (N), Sulphur (S), and other data on the dry basis, while Oxygen (O) fraction is the difference between 100% and mass fraction of elements.

Data from Tables 2 and 1 are also the input for the gasification calculation in the next step.

Table 1
Assumed gasification conditions.

Parameter	Symbol	Unit	Value
Gasification temperature	T	K	1033.15
	t	°C	760
Gasification pressure	p	atm	1
Sewage Sludge inlet temperature	t_{ss}	°C	70
Converter inlet temperature	t_{con}	°C	96
Converter H_2O mole fraction	x_{H_2O}	mol%	100

2.2. Overview on modelling approaches

Identification of feasible ways of sewage sludge gasification can be treated as an introduction to the design stage of a gasifying system. Feasibility study of gasification process along with experimental sewage sludge gasification requires certain estimations. In general, simulation methods of gasification are based on mass, energy, and momentum conservation. A distinction is made between the following modelling approaches in particular: thermodynamic equilibrium, kinetic, Computational Fluid Dynamics (CFD), and

Table 2
Proximate and ultimate analysis of sewage sludge used.

Specification	Unit	Value
Fixed Carbon	$\%_{dry}$	9.40
Volatile Matter	$\%_{dry}$	58.10
Ash	$\%_{dry}$	32.50
Moisture content[a]	$\%_{wb}$	2.00
HHV	MJ/kg	15.70
C	$\%_{dry}$	27.89
H	$\%_{dry}$	6.67
N	$\%_{dry}$	4.36
S	$\%_{dry}$	0.29
O[b]	$\%_{dry}$	28.29

[a] – assumed value, after drying of sewage sludge.
[b] – determined by difference.

Machine Learning (ML). Continuous development of diverse methods does not impose one's own model selection. Therefore, each approach, depending on the required accuracy of the results, can be used for different purposes such as feasibility study, design or optimisation [68–70]. Thermodynamic equilibrium models basically are zero-dimensional gasifying reactor models based on simplifying assumptions such as steady-state, infinite residence time, and neglect char or tar formation. This modelling approach can be further identified as a stoichiometric model [71] that is based on the equilibrium constants of chemical reactions or a non-stoichiometric model that is based on the minimalization of the Gibbs free energy [71,72]. Outcomes of equilibrium models reflect the potential of the gasifying system, which is close to ideal conditions. Because of nonequilibrium factors inside the gasifying reactor, the results of the model are usually divergent from the experiment. In most cases, equilibrium models underestimate CH_4 and CO_2 content while overestimating CO and H_2 in the syngas. For accurate prediction of real conditions, the inclusion of empirical correction factors derived from experiments is required. Modified equilibrium models can also be extended into multi-dimensionality [69,73–81]. Kinetic models are based on the kinetics of key reactions in the process. In contrary to the equilibrium method, the process is computed for a fixed amount of time that translates to accurate results, but this method is complex. Kinetic models are usually multidimensional models which are composed of computational stages, each representing a different section of the gasifying unit, essentially useful for the design of a gasifying system [68,79,82].

The machine learning (ML) methods used for the gasification process are based on regression technique analysis. Analysis can be conducted by sophisticated non-interpretable models, for example, some types of ANN or Support Vector Machines, and interpretable models, for example, Linear Regression or Decision Tree Regressors. Since these models must be trained and validated with dedicated experimental data from an already built gasifier, thus each developed ML model is treated as unique. To produce accurate results, such a model requires a large amount of data. Therefore, ML models can be successfully used for optimisation tasks [68,83]. CFD is an effective modelling tool to study the process of the gasifying reactor. While the aforementioned methods focus on the gasification process rather holistically, CFD methods produce fluid behaviour in greater detail. Gasifiers involve complex physical and chemical phenomena, including fluid flow, heat and mass transfer, and chemical reactions. Combined with data from existing pilot and commercial-scale gasifiers, CFD models offer a powerful method for understanding and improving gasification systems. CFD modelling can provide insights into the flow field within the gasifier, which can be used to enhance its design, analysis, and operation [68,84].

2.3. Model selection

For the feasibility study of sewage sludge gasification, the modified thermodynamic equilibrium model was developed. This quasi-equilibrium model is primarily based on the stoichiometric thermodynamic equilibrium method, namely, the Deringer method with Gumz modification. The modification was made with the inclusion of tuned equilibrium constants, which were empirically determined, quasi-temperatures derived from energy balance conservation, and the use of iterative algorithm code [78]. This quasi-equilibrium model provides results for any given fuel composition, converter composition, temperature, or pressure. Applied code immediately iterates the range of specified parameters one after another in a relatively short period of time.

2.3.1. Chemical reactions

The gasification process can be represented by the global reaction formula as follows:

$$C_aH_bO_cN_dS_eAsh_X(H_2O)_M + f(con.) \xrightarrow{t} hCO_2 + iH_2 + jCO + kN_2 + lSO_2 + mC_3H_8 + nCH_4 + oH_2O + XAsh \quad (2)$$

where:

a, b, c, d, e, X, M – molar masses of elements and components per 1 kg of feedstock in [mol/kg],

f – required molar mass of converter components to gasify 1 kg of feedstock in [mol/kg],

h, i, j, k, l, m, n, o – molar masses of syngas components after gasification 1 kg of feedstock in [mol/kg],

t – gasification temperature in [°C].

Given is the feedstock composition a, b, c, d, e, X, M and gasification temperature t, while the unknowns are the amount of gasifying agent f and the number of syngas ingredients h, i, j, k, l, m, n, o. Char and tar formation is neglected. The following chemical reactions in gasification are taken into account, and their corresponding equilibrium constants are determined to quantify the chemical equilibria, where the right side of the reaction indicating its direction is always in the counter of the equilibrium constant equation. For the equilibrium equation of each reaction, only the gaseous phase component mole fractions are taken into account [78,85,86]:

- Boudouard reaction:

$$C + CO_{2(g)} = 2CO_{(g)}$$
$$K_{(1)} = \frac{x_{CO}^2}{x_{CO_2}} p \quad (3)$$

where:

p – pressure of the process in [atm],

x_{CO}, x_{CO2} – molar fraction of CO, CO_2 in [%mol].

- Water-gas reaction:

$$C + H_2O_{(g)} = CO_{(g)} + H_{2(g)}$$
$$K_{(2)} = \frac{x_{CO} \cdot x_{H_2}}{x_{H_2O}} p \quad (4)$$

where:

x_{H_2}, x_{H_2O} – molar fraction of H_2, H_2O in [%mol].

- Formation reaction for methane:

$$C + 2H_{2(g)} = CH_{4(g)}$$
$$K_{(3)} = \frac{x_{CH_4}}{x_{H_2}^2} \cdot \frac{1}{p} \quad (5)$$

where:
x_{CH_4} – molar fraction of CH_4 in [%mol].

- Water-gas shift reaction:

$$CO_{2(g)} + H_{2(g)} = CO_{(g)} + H_2O_{(g)}$$
$$K_{(4)} = \frac{x_{CO} \cdot x_{H_2O}}{x_{CO_2} \cdot x_{H_2}} \quad (6)$$

- Formation reaction for propane:

$$3C + 4H_{2(g)} = C_3H_{8(g)}$$
$$K_{(5)} = \frac{x_{C_3H_8}}{x_{H_2}^4} \cdot \frac{1}{p^3} \quad (7)$$

where:
$x_{C_3H_8}$ – molar fraction of C_3H_8 in [%mol].

2.3.2. Equilibrium constants estimation

Equilibrium constants, namely $K_{(1)}$, $K_{(2)}$, $K_{(3)}$, $K_{(4)}$, $K_{(5)}$ are unknown. There are different models to calculate these equilibrium constants ranging from very detailed to simplified methods and those that were approximately tailored to resemble the real conditions, for example [78,87]:

- Computational methods,
- Experimental methods,
- Ulich approximate method,
- Tymkin-Schwartzman method,
- Nernst approximate method,
- Approximated equations, e.g., Gumz approximations.

A model based on approximated equations is acceptable when the data are fitted within the experimental error. For the gasification model, the equilibrium constants approximation derived by Gumz [87] will be used, except for the propane formation equilibrium constant, which is obtained from Nernst approximate method [78]. Approximations are based on the assumption that equilibrium constants may be corrected by considering multiplicative factors to account for the actual distance of a real gasifier from the ideal equilibrium state [87].

$$K_{(1)} = 10^{\left(3.26730 - \frac{8820.690}{T} - 1.208714 \cdot 10^{-3} T + 0.153734 \cdot 10^{-6} \cdot T^2 + 2.295483 \cdot lgT\right)}$$

$$K_{(2)} = 10^{\left(0.8255488 \cdot 10^{-6} \cdot T^2 + 14.515670 \cdot lgT - \frac{4825.986}{T} - 5.671122 \cdot 10^{-3} \cdot T - 33.45778\right)}$$

$$K_{(3)} = 10^{\left(\frac{4662.80}{T} - 2.09594 \cdot 10^{-3} T + 0.38620 \cdot 10^{-6} T^2 + 3.034338 \cdot lgT - 13.06361\right)}$$

$$K_{(4)} = 10^{\left(3672508 - \frac{3994.704}{T} + 4.462408 \cdot 10^{-3} T - 0.671814 \cdot 10^{-6} \cdot T^2 - 12.220277 \cdot lgT\right)}$$

For the propane formation, the Nernst approximate method was adopted [78].

$$K_{(5)} = 10^{\left(-2.96 - 14.143 \cdot lgT + \frac{5427.7}{T}\right)} \quad (8)$$

2.3.3. Formulas to calculate mole amount of elements in fuel and converter

In the next step, the mole number of elements per 1 kmol of feedstock and per 1 kmol of gasifying agent (converter) is calculated. Feedstock ingredients such as carbon, hydrogen, oxygen, nitrogen, sulphur, moisture, and converter ingredients such as air, steam, carbon dioxide, and moisture are taken into account [78,87]:

$$
\begin{aligned}
(C)_{fuel} &= \frac{C}{M_C}\cdot M_{fuel}\left[\frac{kmol\,C}{kmol\,fuel}\right]\\
(C)_{con} &= \frac{\gamma_{CO_2}}{1+\beta_{steam}+\gamma_{CO_2}}\ or\ (C)_{con} = x_{CO_2}^{con}\left[\frac{kmol\,C}{kmol\,con.}\right]\\
(H)_{fuel} &= \left(\frac{H}{M_{H_2O}} + 2\cdot\frac{w_{fuel}}{M_{H_2O}}\right)\cdot M_{fuel}\left[\frac{kmol\,H}{kmol\,fuel}\right]\\
(H)_{con} &= \frac{2\cdot\left(\beta_{steam}+\dfrac{0.79\cdot M_{N_2}+0.21\cdot M_{O_2}}{M_{H_2O}}X_{air}\right)}{1+\beta_{steam}+\gamma_{CO_2}}\ or\ (H)_{con} = 2\cdot x_{H_2O}^{con}\left[\frac{kmol\,H}{kmol\,con.}\right]\\
(O)_{fuel} &= \left(\frac{O}{M_O}+\frac{w_{fuel}}{M_{H_2O}}\right)\cdot M_{fuel}\left[\frac{kmol\,O}{kmol\,fuel}\right]\\
(O)_{con} &= \frac{2\cdot\left(\left(1-\dfrac{0.79\cdot M_{N_2}+0.21\cdot M_{O_2}}{M_{H_2O}}X_{air}\right)\cdot 0.21+\gamma_{CO_2}\right)+\beta_{steam}}{1+\beta_{steam}+\gamma_{CO_2}}\left[\frac{kmol\,O}{kmol\,con.}\right]\\
or\ (O)_{con} &= 2\cdot\left(x_{O_2}^{con}+x_{CO_2}^{con}\right)+x_{H_2O}^{con}\left[\frac{kmol\,O}{kmol\,con.}\right]\\
(N)_{fuel} &= \frac{N}{M_N}\cdot M_{fuel}\left[\frac{kmol\,N}{kmol\,fuel}\right]\\
(N)_{con} &= \frac{2\cdot\left(1-\dfrac{0.79\cdot M_{N_2}+0.21\cdot M_{O_2}}{M_{H_2O}}X_{air}\right)\cdot(1-0.21)}{1+\beta_{steam}+\gamma_{CO_2}}\\
or\ (N)_{con} &= 2\cdot x_{N_2}^{con}\left[\frac{kmol\,N}{kmol\,con.}\right]\\
(S)_{fuel} &= \frac{S}{M_S}\cdot M_{fuel}\left[\frac{kmol\,S}{kmol\,fuel}\right]\\
(S)_{con} &= 0\left[\frac{kmol\,S}{kmol\,con.}\right]
\end{aligned}
\tag{9}
$$

The molar mass of the feedstock fuel:

$$M_{fuel} = \left(\frac{C}{M_C}+\frac{H}{M_{H_2}}+\frac{O}{M_{O_2}}+\frac{N}{M_{N_2}}+\frac{S}{M_S}+\frac{w_{fuel}}{M_{H_2O}}\right)^{-1}\left[\frac{kg\,fuel}{kmol\,fuel}\right]$$

And the molar mass of the converter:

$$M_{con} = x_{CO_2}^{con}\cdot M_{CO_2} + x_{H_2O}^{con}\cdot M_{H_2O} + x_{O_2}^{con}\cdot M_{O_2} + x_{N_2}^{con}\cdot M_{N_2}\left[\frac{kg\,con.}{kmol\,con.}\right]$$

where:

C, H, O, N, S – mass fractions of elements in the feedstock.

M_C, M_{H_2}, M_{H_2O}, M_{O_2}, M_{N_2}, M_S – molar masses of particular ingredients.

M_H, M_O, M_N – molar masses of elements in the feedstock in [kg/kmol],

w_{fuel} – moisture mass fraction in the feedstock.

X_{air} – moisture mass content related to dry air.

β_{steam} – steam to dry air mole factor in the converter.

γ_{CO_2} – CO_2 to dry air mole factor in the converter.

$x_{CO_2}^{con}$, $x_{H_2O}^{con}$, $x_{O_2}^{con}$, $x_{N_2}^{con}$ – molar fractions of gasifying agent ingredients in [%mol].

2.3.4. Deringer-Gumz equilibrium method

Deringer with Gumz modification equilibrium method for syngas calculation during gasification is presented below. This method was initially destined for coal feedstock composed of only carbon elements, but the Gumz modification allows analysing fuels with various compositions, including sulphur compounds in the producer gas. The source of the presented formulas is the books by Kozaczka [78], where over a dozen of equilibrium methods were elaborated. Equations of Deringer-Gumz, as well as other equilibrium methods, are solved by iterative techniques. The number of formulas for the Deringer-Gumz description is much shortened in comparison to Kozaczka [78] or Gumz [87], which was achieved by applying the code written in Microsoft Visual Basic for iterative calculations instead of manual calculations. Deringer with Gumz modification method does not include the inlet temperature of the converter and the inlet temperature of the feedstock. Therefore, the energy balance, including these temperatures, has to be solved in the additional step. The scheme showing the calculation process is shown in Fig. 2 [78,87]. The method is based on the balanced equation of syngas components which follows the Dalton law:

$$x_{CO} + x_{CO_2} + x_{H_2} + x_{H_2O} + x_{CH_4} + x_{N_2} + x_{C_3H_8} + x_{SO_2} = 1 \tag{10}$$

Calculations required in the procedure shown in Fig. 2 are as follows:

- Iterative estimation of a ratio

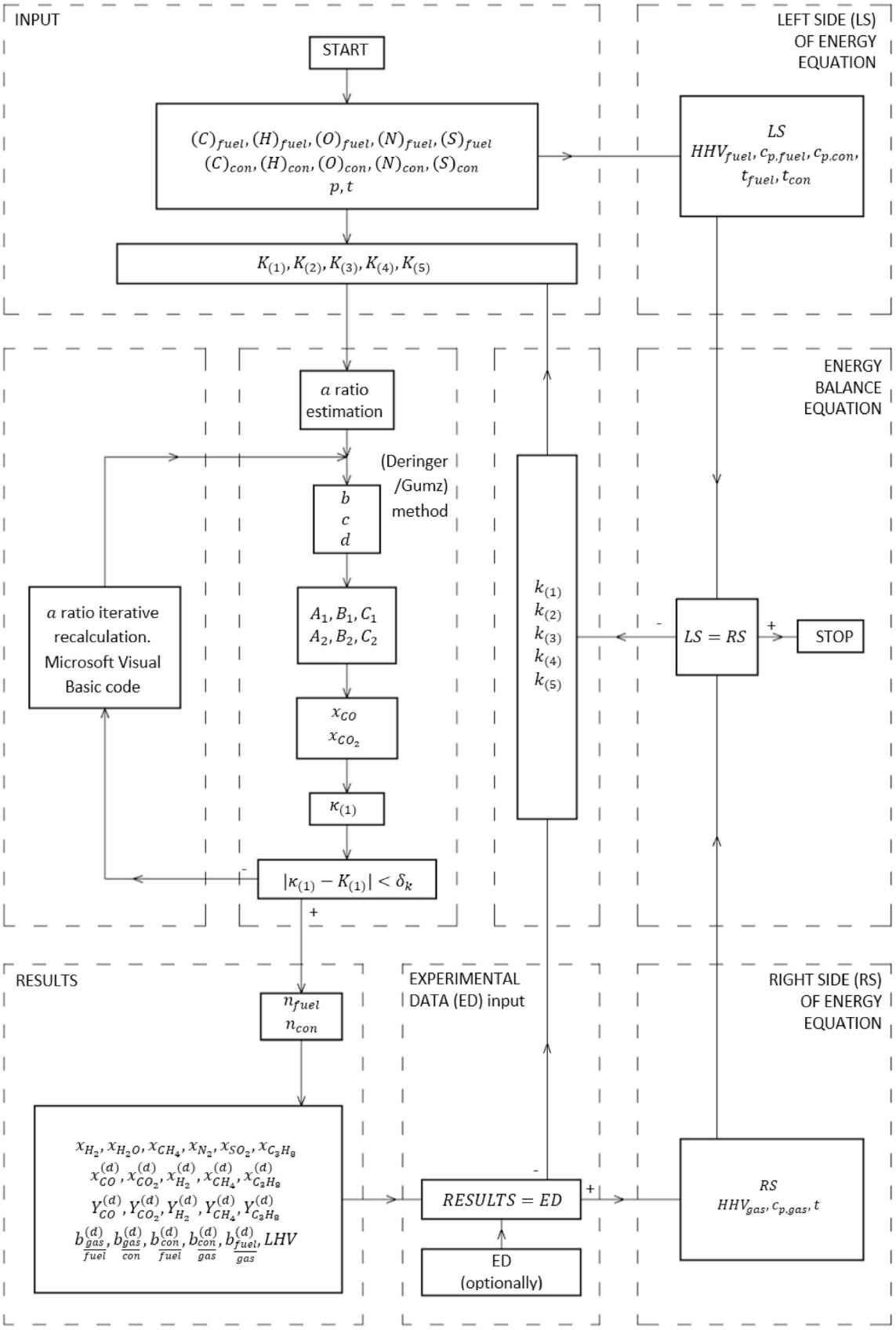

Fig. 2. Diagram for calculating gasification process by the Deringer method with the Gumz modification with included energy balance equation that is essential for the verification purpose.

$$a = \frac{x_{H_2}}{x_{CO}} \tag{11}$$

- Determination of CO and CO_2 molar fractions of syngas. These equations are modified in comparison to the Deringer model, and they are a result of the Dalton law.

$$x_{CO_2} = \frac{(A_2 - C_1)\cdot\left(B_1 - \frac{A_1\cdot B_2}{A_2} - \sqrt{\left(B_1 - \frac{A_1\cdot B_2}{A_2}\right)^2 + 4\cdot\left(C_1 - \frac{A_1\cdot C_2}{A_2}\right)}\right)}{2\cdot\frac{A_1\cdot C_2}{A_2} - C_2}\ [\%mol] \quad x_{CO} = \frac{1 - B_1\cdot x_{CO_2} - C_1\cdot x_{CO_2}^2}{A_1}\ [\%mol] \tag{16}$$

- Assignation of b, c, d auxiliary ratios. Ratio d is a new modification to the original model and is related to propane formation

$$b = a^2\cdot K_{(1)}\cdot K_{(3)} \quad c = a\cdot K_{(4)} \quad d = a^4\cdot K_{(5)}\cdot K_{(1)}^2\cdot p \tag{12}$$

- Reduced balance of particular elements, to include elements of sulphur dioxide in the model, which is treated as an inert compound, the same as nitrogen. The inclusion of sulphur dioxide is a new modification to the original model

$$\begin{aligned}
(OS)_{con} &= (O)_{con} - 2\cdot(S)_{con}\left[\frac{kmol}{kmol\ con.}\right]\\
(NS)_{con} &= (N)_{con} + (S)_{con}\left[\frac{kmol}{kmol\ con.}\right]\\
(OS)_{fuel} &= (O)_{fuel} - 2\cdot(S)_{fuel}\left[\frac{kmol}{kmol\ fuel}\right]\\
(NS)_{fuel} &= (N)_{fuel} + (S)_{fuel}\left[\frac{kmol}{kmol\ fuel}\right]
\end{aligned} \tag{13}$$

- Calculating criterial parameter $\kappa_{(1)}$ derived from iterations of a ratio, which must be almost equal to the target equilibrium constant $K_{(1)}$

$$\kappa_{(1)} = \frac{x_{CO}}{x_{CO_2}} \tag{17}$$

- thus, the program is set to achieve accurate results after completing iterations when the following condition is met

$$\left|\kappa_{(1)} - K_{(1)}\right| < \delta_k \tag{18}$$

where:

- Evaluation of k_1, k_2, k_3, k_4 relations, including reduced balances.

δ_k – permissible error.[1]

2.3.5. Formulas to obtain results from the model

$$k_1 = \frac{1}{2}\frac{(OS)_{con}\cdot(NS)_{fuel} - (OS)_{fuel}\cdot(NS)_{con}}{(C)_{fuel}\cdot(OS)_{con} - (C)_{con}\cdot(OS)_{fuel}} \quad k_2 = \frac{1}{2}\frac{(C)_{fuel}\cdot(NS)_{con} - (CS)_{con}\cdot(NS)_{fuel}}{(C)_{fuel}\cdot(OS)_{con} - (C)_{con}\cdot(OS)_{fuel}} \quad k_3 = \frac{(C)_{con}\cdot(H)_{fuel} - (C)_{fuel}\cdot(H)_{con}}{(C)_{con}\cdot(OS)_{fuel} - (C)_{fuel}\cdot(OS)_{con}}$$
$$k_4 = \frac{(OS)_{fuel}\cdot(H)_{con} - (OS)_{con}\cdot(H)_{fuel}}{(C)_{con}\cdot(OS)_{fuel} - (C)_{fuel}\cdot(OS)_{con}} \tag{14}$$

- Evaluation of A_1, B_1, C_1, A_2, B_2, C_2 equations, where C_1, C_2 are new to the original model related to the inclusion of propane formation.

- Required mole amount of feedstock fuel and converter per 1 kmol of syngas

$$A_1 = 1 + a + k_1 + k_2 \quad B_1 = 1 + b + c + (1 + b)\cdot k_1 + (2 + c)\cdot k_2 \quad C_1 = d + 3\cdot k_1\cdot d \quad A_2 = k_3 + k_4 - 2\cdot a$$
$$B_2 = (2 + c)\cdot k_3 + (1 + b)\cdot k_4 - 4\cdot b - 2\cdot c \quad C_2 = 3\cdot k_4\cdot d - 8\cdot d \tag{15}$$

[1] Assumed permissible error $\delta_k = 0.0001$.

$$n_{fuel} = \frac{(C)_{con} - (OS)_{con}}{(C)_{con}\cdot(OS)_{fuel} - (CS)_{fuel}\cdot(OS)_{con}}\cdot x_{CO} + \frac{(2+c)\cdot(C)_{con} - (1+b)\cdot(OS)_{con}}{(C)_{con}\cdot(OS)_{fuel} - (C)_{fuel}\cdot(OS)_{con}}\cdot x_{CO_2} - \frac{3\cdot d\cdot(OS)_{con}}{(C)_{con}\cdot(OS)_{fuel} - (C)_{fuel}\cdot(OS)_{con}}\cdot x_{CO_2}^2 \left[\frac{kmol\ fuel}{kmol\ gas}\right]$$

$$n_{con} = \frac{(OS)_{fuel} - (C)_{fuel}}{(C)_{con}\cdot(OS)_{fuel} - (C)_{fuel}\cdot(OS)_{con}}\cdot x_{CO} + \frac{(1+b)\cdot(OS)_{fuel} - (2+c)\cdot(C)_{fuel}}{(C)_{con}\cdot(OS)_{fuel} - (C)_{fuel}\cdot(OS)_{con}}\cdot x_{CO_2} + \frac{3\cdot d\cdot(OS)_{fuel}}{(C)_{con}\cdot(OS)_{fuel} - (C)_{fuel}\cdot(OS)_{con}}\cdot x_{CO_2}^2 \left[\frac{kmol\ con.}{kmol\ gas}\right] \quad (19)$$

$$x_{H_2} = a\cdot x_{CO}\ [\%mol] \quad x_{CH_4} = b\cdot x_{CO_2}[\%mol] \quad x_{C_3H_8} = d\cdot x_{CO_2}^2[\%mol] \quad x_{H_2O} = c\cdot x_{CO_2}[\%mol] \quad x_{SO_2} = n_{fuel}\cdot(S)_{fuel} + n_{con}\cdot(S)_{con}[\%mol]$$

$$x_{N_2} = (k_1+k_2)\cdot x_{CO} + ((1+b)\cdot k_1 + (2+c)\cdot k_2)\cdot x_{CO_2} + 3\cdot d\cdot k_1\cdot x_{CO_2}^2 - \frac{x_{SO_2}}{2}[\%mol] \quad (20)$$

- Calculation of other syngas components mole fractions obtained from computational gasification

Molar fractions of normalized components for dry, clean gas ($x_{H_2O} = 0$, $x_{SO_2} = 0$, $x_{N_2} = 0$):

$$x_{CO}^{(d)} = \frac{x_{CO}}{1 - x_{H_2O} - x_{SO_2} - x_{N_2}}\ [\%mol] \quad x_{CO_2}^{(d)} = \frac{x_{CO_2}}{1 - x_{H_2O} - x_{SO_2} - x_{N_2}}\ [\%mol] \quad x_{H_2}^{(d)} = \frac{x_{H_2}}{1 - x_{H_2O} - x_{SO_2} - x_{N_2}}\ [\%mol]$$
$$x_{CH_4}^{(d)} = \frac{x_{CH_4}}{1 - x_{H_2O} - x_{SO_2} - x_{N_2}}\ [\%mol] \quad x_{C_3H_8}^{(d)} = \frac{x_{C_3H_8}}{1 - x_{H_2O} - x_{SO_2} - x_{N_2}}\ [\%mol] \quad (21)$$

The molar mass of dry and cleaned gas with normalized components:

$$M_{gas}^{(d)} = x_{CO}^{(d)}\cdot M_{CO} + x_{CO_2}^{(d)}\cdot M_{CO_2} + x_{H_2}^{(d)}\cdot M_{H_2} + x_{CH_4}^{(d)}\cdot M_{CH_4} + x_{C_3H_8}^{(d)}\cdot M_{C_3H_8}\left[\frac{kg\ dry\ gas}{kmol\ dry\ gas}\right] \quad (22)$$

Dry gas mass fractions

$$Y_{CO}^{(d)} = \frac{x_{CO}^{(d)}\cdot M_{CO}}{M_{gas}^{(d)}} \quad Y_{CO_2}^{(d)} = \frac{x_{CO_2}^{(d)}\cdot M_{CO_2}}{M_{gas}^{(d)}} \quad Y_{H_2}^{(d)} = \frac{x_{H_2}^{(d)}\cdot M_{H_2}}{M_{gas}^{(d)}} \quad Y_{CH_4}^{(d)} = \frac{x_{CH_4}^{(d)}\cdot M_{CH_4}}{M_{gas}^{(d)}} \quad Y_{C_3H_8}^{(d)} = \frac{x_{C_3H_8}^{(d)}\cdot M_{C_3H_8}}{M_{gas}^{(d)}} \quad (23)$$

- Mass of dry and cleaned gas derived from 1 kmol of total product gas ($x_{H_2O} = 0$, $x_{SO_2} = 0$, $x_{N_2} = 0$):

$$b_{\frac{gas}{gas}}^{(d)} = x_{CO}\cdot M_{CO} + x_{CO_2}\cdot M_{CO_2} + x_{H_2}\cdot M_{H_2} + x_{CH_4}\cdot M_{CH_4} + x_{C_3H_8}\cdot M_{C_3H_8}\left[\frac{kg\ dry\ gas}{kmol\ gas}\right] \quad (24)$$

- Mass of dry and cleaned gas obtained from 1 kg of feedstock gasification, formula including CO_2 from the gasifying agent is the following

$$b_{\frac{gas}{fuel}}^{(d)} = \frac{b_{\frac{gas}{gas}}^{(d)}}{\left(x_{CO_2} + x_{CO} + x_{CH_4} + 3\cdot x_{C_3H_8} - n_{con}\cdot x_{CO_2}^{con}\right)}\cdot\frac{C}{M_C}\left[\frac{kg\ gas}{kg\ fuel}\right]$$

or

$$b_{\frac{gas}{fuel}}^{(d)} = \frac{b_{\frac{gas}{gas}}^{(d)}}{M_{fuel}\cdot n_{fuel}}\left[\frac{kg\ gas}{kg\ fuel}\right] \quad (25)$$

- Mass of dry and cleaned gas obtained from 1 kg of gasifying agent

$$b_{\frac{gas}{con}}^{(d)} = \frac{b_{\frac{gas}{gas}}^{(d)}}{M_{con}\cdot n_{con}}\left[\frac{kg\ gas}{kg\ con.}\right] \quad (26)$$

- Required mass of the converter per 1 kg of the fuel feedstock during gasification

$$b_{\frac{con}{fuel}} = \frac{M_{con}\cdot n_{con}}{M_{fuel}\cdot n_{fuel}}\left[\frac{kg\ con.}{kg\ fuel}\right] \quad (27)$$

- Required converter mass per 1 kg of dry and cleaned gas

$$b_{\frac{con}{gas}}^{(d)} = b_{\frac{gas}{con}}^{(d)\,-1}\left[\frac{kg\ con.}{kg\ gas}\right] \tag{28}$$

- Required fuel feedstock mass per 1 kg of dry and cleaned gas

$$b_{\frac{fuel}{gas}}^{(d)} = b_{\frac{gas}{fuel}}^{(d)\,-1}\left[\frac{kg\ fuel}{kg\ gas}\right] \tag{29}$$

- Calculating LHV and HHV at 25 °C

$$\begin{aligned}
&C_aH_bO_c + (a\ +\ ¼b\ -\ ½c)\cdot O_2 \rightarrow a\cdot CO_{2(g)} + ½b\cdot H_2O_{(l)} + HHV\\
&HHV_{(C_aH_bO_c)} = -a\cdot\Delta H_f^0(CO_2,g)\ -\ ½b\cdot\Delta H_f^0(H_2O,l)\ +\ \Delta H_f^0\cdot(C_aH_bO_c)\ +\ (a\ +\ ¼b\ -\ ½c)\cdot\ \Delta H_f^0(O_2,g)\\
&LHV_{(C_aH_bO_c)} = -a\cdot\Delta H_f^0(CO_2,g)\ -\ ½b\cdot\Delta H_f^0(H_2O,g)\ +\ \Delta H_f^0\cdot(C_aH_bO_c)\ +\ (a\ +\ ¼b\ -\ ½c)\cdot\ \Delta H_f^0(O_2,g)\\
&LHV_{gas} = HHV_{CO} + LHV_{H_2} + LHV_{CH_4} + LHV_{C_3H_8}\\
&HHV_{gas} = HHV_{CO} + HHV_{H_2} + HHV_{CH_4} + HHV_{C_3H_8}
\end{aligned} \tag{30}$$

where ΔH_f^0 is the enthalpy of formation for a given substance at standard conditions (25 °C, 1 bar).

$$\theta = \frac{LHV_{gas}}{LHV_{fuel}} \tag{31}$$

- Cold gas yield

2.3.6. Energy balance equation

Energy balance (for checking purposes) [78]:

$$\begin{aligned}
LS = RS\quad & n^{fuel}\cdot HHV^{fuel} + T\cdot\left(n^{fuel}\cdot c_p^{fuel} + n^{con}\cdot c_p^{con}\right)\\
& = HHV^{gas} + i^{gas} + Q_V
\end{aligned} \tag{32}$$

where:

n^{fuel} – fuel amount in [kmol fuel/kmol gas],
n^{con} – gasifying agent amount in [kmol con/kmol gas],
i^{gas} – specific enthalpy of gas in [kJ/kmol gas],
c_p^{fuel} – specific heat of fuel in [kJ/kmol gas K],
c_p^{con} – specific heat of gasifying agent in [kJ/kmol gas K],
HHV^{fuel} – specific higher heating value of fuel in [kJ/kmol gas],
HHV^{gas} – specific higher heating value of gas in [kJ/kmol gas],
Q_V – specific energy losses, including ash in [kJ/kmol gas].

- Specific heat of feedstock

For the case of the heat capacity, the c_p value of the sewage sludge is missing. It could be calculated using two methods. Using the formula obtained experimentally for the sewage sludge by Arlabosse et al. [88] or the formula for inorganic substances, based on Appendix in Kozaczka reference [78], using dry and ash-free data. Combining both of these formulas will complement each other, as the first formula is focused on sewage sludge in general (including ash), and the second one focuses only on chemical elements without ash but is dedicated to inorganic compounds, while the introduced sewage sludge sample has 58,1%$_{db}$ of Volatile Matter (56,94%$_{wb}$) is a rough estimation of the organic fraction. Further exploration of the sewage sludge heat capacity and its ash separately, including the ash composition, is recommended. High diversity of ash content between various samples is to be expected.

a. Version 1, dry basis [88]:

$$c_p^{fuel} = (1434 + 3.29\cdot T)\cdot M_{dry\ fuel} \tag{33}$$

b. Version 2, dry ash-free [78]:

$$\begin{aligned}
c_p^{fuel} = {} & C\cdot c_{p,C(g)}(T) + H\cdot c_{p,H(g)}(T) + O\cdot c_{p,O(g)}(T) + N\cdot c_{p,Ng(g)}(T)\\
& + S\cdot c_{p,S(g)}(T)
\end{aligned} \tag{34}$$

3. Results and discussion

To prove that the results obtained from the presented model based on the Deringer-Gumz-modification method were calculated properly, the original model produced very similar results to examples solved by a dozen other equilibrium methods described in Kozaczka [78], such as the "Traustel Newtonian approximation" method or "Deringer with Traustel extension" method.

New model results were adjusted to the experimental results for the temperature of 760 °C by tuning the $K_{(1)}$, $K_{(3)}$, $K_{(4)}$, $K_{(5)}$ equilibrium constants using an approximation approach by $k_{(1)}$, $k_{(3)}$, $k_{(4)}$, $k_{(5)}$ coefficients multiplication, where $k_{(1)}$ is equal to 0.00224, $k_{(3)}$ equal to 19.3, $k_{(4)}$ equal to 1.031, and $k_{(5)}$ equal to $8.97*10^{27}$. The results for other temperatures were extrapolated. Future experimental gasification with plasma will be done at the temperature of 1300 °C, thus extrapolated results for this temperature are additionally presented. According to formula (2), the conversion of 1 kg sewage sludge to syngas at the temperature of 760 °C and 1300 °C (extrapolation) is the following:

The inputs for the calculation were the values presented in

$$C_{22.7}H_{64.8}O_{17.3}N_{3.1}S_{0.1}Ash_X(H_2O)_{1.1} + 1\ H_2O \xrightarrow{760^0C}$$
$$0.29\ CO + 0.99CO_2 + 2.09\ H_2 + 0.15\ N_2 + 0.01\ SO_2 + 0.14\ C_3H_8 + 0.57\ CH_4 + 6.1\ H_2O + XAsh$$

$$C_{22.7}H_{64.8}O_{17.3}N_{3.1}S_{0.1}Ash_X(H_2O)_{1.1} + 1\ H_2O \xrightarrow{extrapolation\ 1300^0C}$$
$$2.1\ CO + 0.1\ CO_2 + 3.68\ H_2 + 0.15\ N_2 + 0.01\ SO_2 + 0.001\ C_3H_8 + 0.07\ CH_4 + 0.54\ H_2O + XAsh$$

Tables 1 and 2, which were used for the experimental setup. As the gasification agent, steam was used. Composition and other data of the calculated syngas fuels for 760 °C and 1300 °C are presented in Table 3. The results of the original model show no agreement with experimental data. However, one may observe a reasonable agreement of the modified model with experimental measurements for the temperature of 760 °C. As regards the mole fraction analysis, for CH_4 and C_3H_8, the agreement is equal to 100%. For CO_2 and H_2, the agreement is equal to 92%, whereas, for CO, it is equal to 76%. As for the LHV of syngas, the level of agreement was equal to 91%. The results prove the credibility and reliability of the approach when estimating the syngas composition after the gasification process. It is also evident that the major %mol component is H_2, with a share of 51.2%. The second major gas component is CO_2, with a share of 24.3%. In order to further assess the credibility of the incorporated approach, the model results for the temperature of 760 °C have been compared with the experimental results of Schweitzer et al. [62], who studied fluidized bed steam gasification of sewage sludge under the temperature of 800 °C. Judging by Fig. 3, one can observe a reasonable agreement of the modified authors' model with the experimental measurements of Schweitzer et al. [62], proving the validity of the former. The differences between the results come from slightly different gasification operating conditions and sewage sludge composition.

After the model extrapolation to 1300 °C, one may notice a substantial increase in the share of CO but also H_2, which contribute

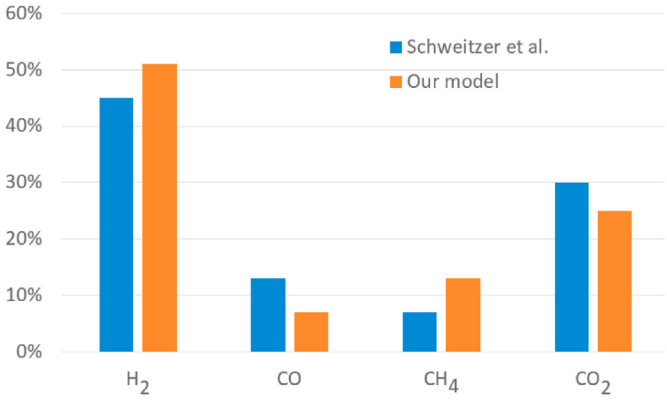

Fig. 3. Comparison of syngas mole composition for our model and literature experimental data [62].

Table 3
Composition of dry and cleaned syngas.

Component	Symbol	Unit	Original model 760 °C	Model 760 °C	Experimental 760 °C	Model extrapolation 1300 °C
CO fraction	$x_{CO}^{(d)}$	%mol	33.8	7.1	9.3	35.3
	$Y_{CO}^{(d)}$	%mass	76.6	11.4	13.7	82.0
CO_2 fraction	$x_{CO_2}^{(d)}$	%mol	2.9	24.3	26.4	1.7
	$Y_{CO_2}^{(d)}$	%mass	10.4	61.1	61.3	6.1
CH_4 fraction	$x_{CH_4}^{(d)}$	%mol	2.4	13.9	13.9	1.2
	$Y_{CH_4}^{(d)}$	%mass	3.1	12.8	11.8	1.6
C_3H_8 fraction	$x_{C_3H_8}^{(d)}$	%mol	–	3.5	3.5	<0.1
	$Y_{C_3H_8}^{(d)}$	%mass	–	8.8	8.1	<0.1
H_2 fraction	$x_{H_2}^{(d)}$	%mol	60.8	51.2	46.8	61.8
	$Y_{H_2}^{(d)}$	%mass	9.9	5.9	5.1	10.3
Lower Heating Value	LHV_{gas}	MJ/kg	21.2	18.7	17.0	21.4
Cold gas yield	θ	%	158	139	–	160
Mass of dry syngas per 1 kg of sewage sludge	$b_{\frac{gas}{fuel}}^{(d)}$	kg	0.72	0.71	–	0.72
Mass of dry syngas per 1 kg of gasifying agent	$b_{\frac{gas}{con}}^{(d)}$	kg	5.59	0.61	–	3.95
Required converter mass per 1 kg of fuel	$b_{\frac{con}{fuel}}$	kg	0.13	1.18	–	0.18
Required converter mass to produce 1 kg of dry syngas	$b_{\frac{con}{gas}}^{(d)}$	kg	0.18	1.65	–	0.25
Required fuel mass to produce 1 kg of dry syngas	$b_{\frac{fuel}{gas}}^{(d)}$	kg	1.39	1.40	–	1.39
Left side of energy equation	LS	MJ/kmol gas	301	192	–	330
Right side of energy equation	RS	MJ/kmol gas	306	189	–	313

to the overall syngas share of 97.1%. At the same time, the share of CO_2 has diminished from 24.3% to 1.7%. Such an outcome can be explained, for instance, by the strong effect of temperature on the gasification reactions. Furthermore, at 1300 °C, there is an increased value of the LHV of syngas equal to 21.4 MJ/kg with respect to 760 °C, where it was equal to 18.7 MJ/kg. Fig. 4 and Fig. 5 are the visualization of Table 3 with respect to the final syngas mass and molar composition, respectively.

Syngas mass chemical composition depending on the gasification temperature is indicated in Fig. 6. One may observe that the mass fractions of CH_4, C_3H_8 and CO_2 have the highest values at lower temperatures. In addition, although the mass fraction of CH_4, CO_2, and C_3H_8 is faced with a decreasing trend in rising temperatures of gasification, increasing the gasification temperature results in the increasing mass fraction of H_2 and CO. One may draw a conclusion that the reactions $C+2H_2 = CH_4$ and $3C+4H_2 = C_3H_8$ have a stronger influence at lower temperatures, whereas at higher temperatures, their impact diminishes, and the effect of $C + CO_2 = 2CO$ and $C + H_2O = CO + H_2$ gasification reactions is even more substantial. Syngas mole chemical composition depending on the gasification temperature is indicated in Fig. 7. From 637 °C, there was a downward trend in the mole fraction of H_2, CH_4, C_3H_8 and CO_2, and it reached a constant value at about 1000 °C. Then, from 637 °C, the mole fraction of CO was faced with an upward trend, and after that, its value remained approximately 30%. Although increasing the temperature causes the mass fraction of CO and H_2 to rise, the decreasing of the mass fraction of CH_4, CO_2, and C_3H_8 results from the rising temperature between 637 °C and 1357 °C.

Fig. 8 depicts the required stack amount of converter and sewage sludge to produce 1 kg of syngas. One may observe that the higher the temperature, the lower amount of the required

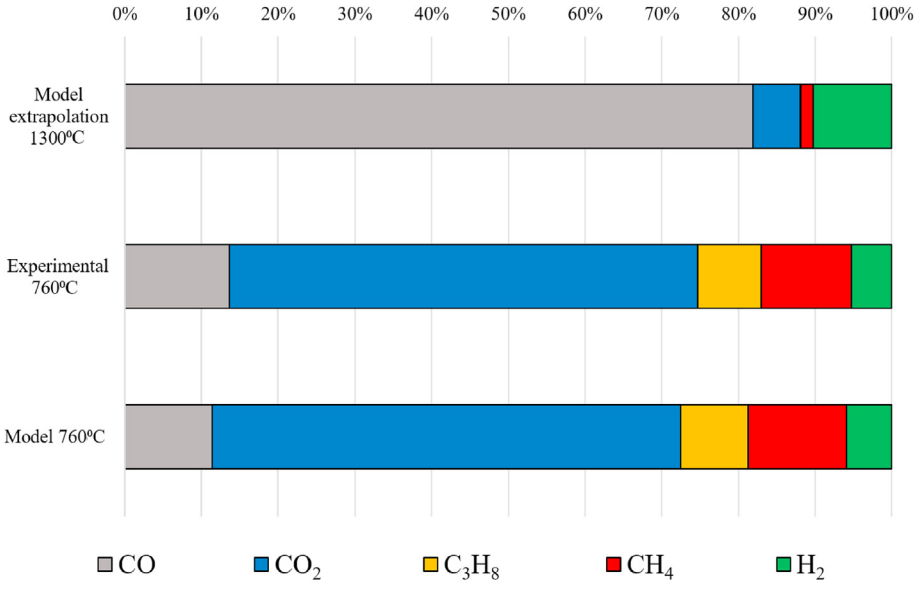

Fig. 4. Comparison of syngas mass composition for model and experiment results.

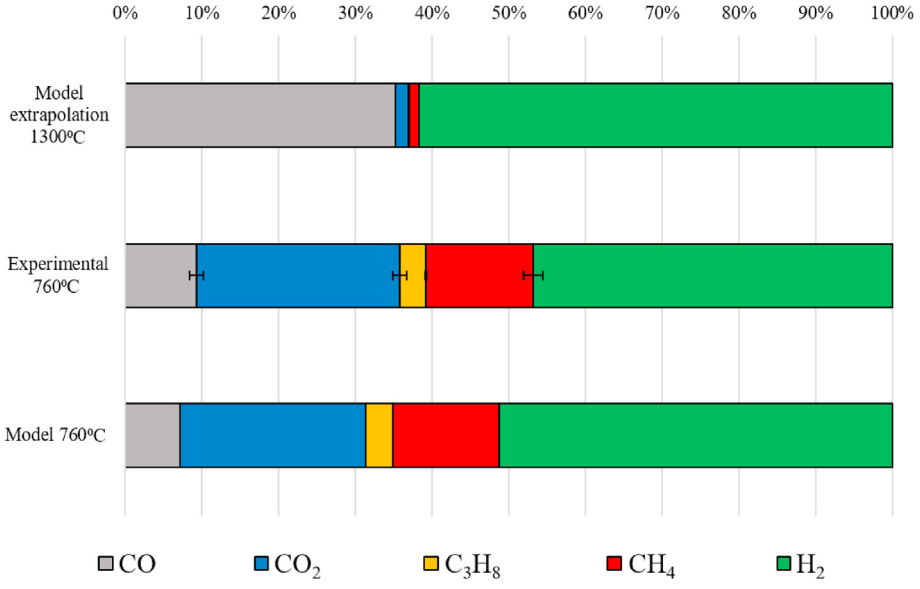

Fig. 5. Comparison of syngas mole composition for model and experiment results.

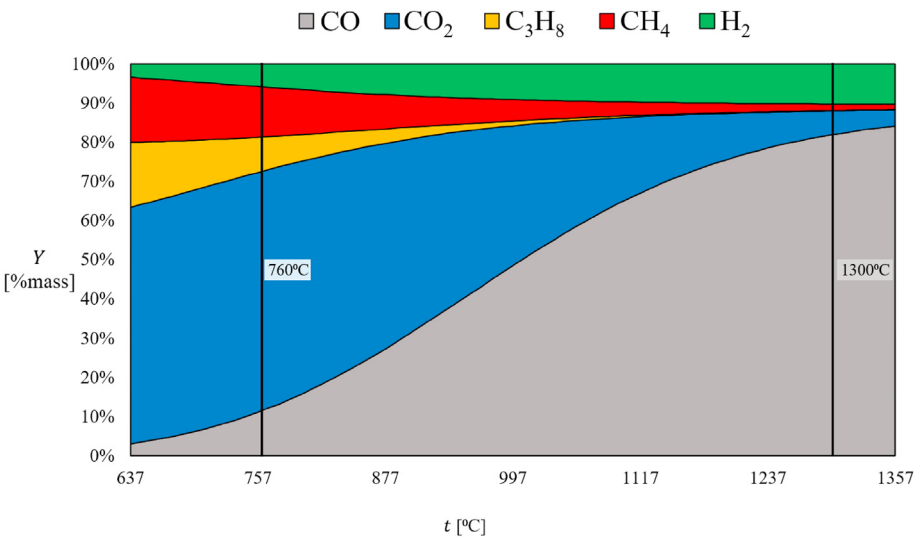

Fig. 6. Model generated syngas mass composition depending on the gasification temperature.

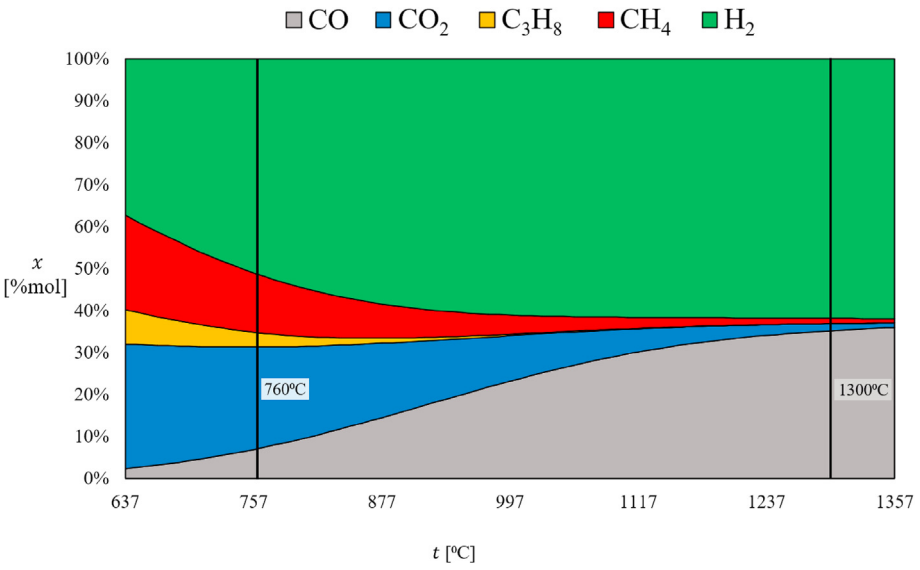

Fig. 7. Model generated syngas mole composition depending on the gasification temperature.

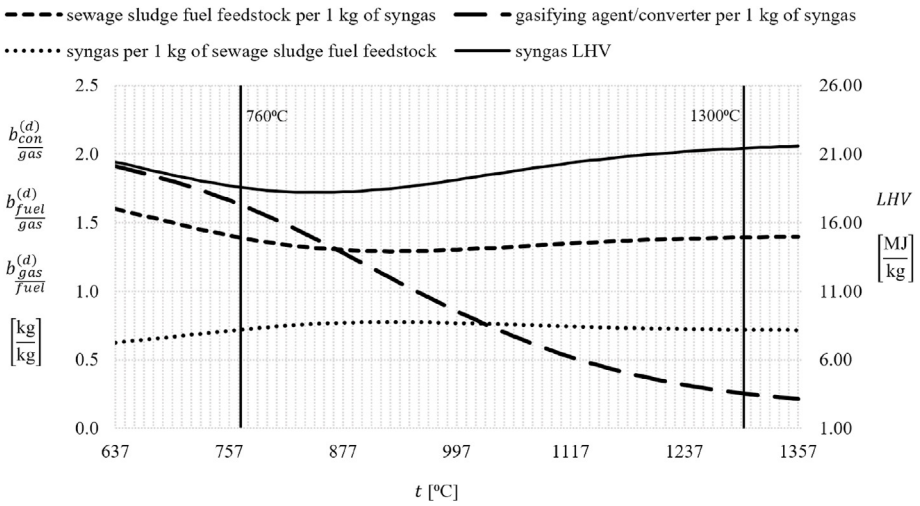

Fig. 8. Model generated required amount of converter and sewage sludge feedstock to produce 1 kg of syngas, produced amount of syngas per 1 kg of sewage sludge fuel feedstock and syngas LHV.

converter/gasifying agent to produce 1 kg of syngas. The higher demand for the converter at lower temperatures results from the direction of temperature-dependent chemical reactions. At lower temperatures, there is more H_2O than H_2 in the wet gas. For 760 °C, there is over 59%mol of H_2O, whereas, for 1300 °C, there is only 8% mol of H_2O. One of the most important issues is the actual technical possibility of achieving high gasification temperatures. Autothermal gasification reactors cannot use steam as the only gasification agent. Sepe et al. [89] reported different configurations of simulations of the steam gasification process, including autothermal reactor (AR) operating at the equivalence ratio (ER) of 0.25 with low-temperature steam (300 K) and steam to carbon ratio equal to 0.125 [89]. The same work investigated high-temperature air gasification (HTAG) using a mixture of air and steam pre-heated to 1500 K (approx.1127 °C) and high-temperature steam gasification (HTSG) using steam at 1400 K (approx.1027 °C) [89]. HTSG resulted in the average temperature of the gasification bed reaching 1050 K (approx. 777 °C) [89]. Lee et al. [90] reported achieving superheated steam at the temperature of 1000 °C, using additional superheaters in electric furnaces [90]. Such a hot gasification agent was used for the gasification of plastics, automobile tire rubber, municipal solid waste (MSW), and woody biomass [90]. The study reported H_2 content varying between 50%$_{vol}$ and 60%$_{vol}$, depending on the feedstock [90]. Nipattummakul et al. [91] performed high-temperature gasification of sewage sludge at the temperature of 900 °C, generating hot steam by stoichiometric combustion of hydrogen, using oxygen [91]. Gasification was performed at laboratory scale, using steam to carbon ratios ranging between 3.05 and 7.38 (mole/mole), resulting in hydrogen contents ranging between 50% $_{vol}$ and 54% $_{vol}$ [91]. However, such ways do give temperatures sufficiently high for vitrification of inorganic fraction of sewage sludge [92]. Vitrification gives a possibility to utilise inorganic residues as a construction material (aggregate) [92], which gives a practical route for achieving end-of-waste status for residues left after thermal treatment of sewage sludge. The use of plasma is a viable way of achieving sufficiently high temperatures due to high energy concentration [65,93]. Diaz et al. [94] performed steam plasma gasification of various types of biomass, achieving a temperature of 3000 °C at the discharge orifice of plasma torch [94].

4. Conclusions

The present paper focused mainly on the in-depth analysis of the modified by authors Deringer-with-Gumz-modification gasification model. It was further compared with the experimental results from allothermal steam gasification. The modification considered above all:

- Gasification reaction for propane which was not found in the literature before
- Equilibrium constants were empirically adjusted
- Sulphur dioxide was applied instead of other sulphur components presented in the original model
- Energy balance equations were introduced
- Reduced amount of equations due to the use of iterative algorithm code.

The proposed model managed to yield highly accurate results in terms of the %mass, and %molar gas composition, and LHV of syngas with respect to the experimental data for the temperature of 760 °C. The results have also been extrapolated to the temperature of 1300 °C. The increase in temperature resulted in a substantial increase in CO and H_2 gas share.

The modification of the model allowed estimation of the concentrations of hydrocarbons with a molar mass higher than methane. Such compounds, usually denoted as C_xH_y, are significant in terms of the influence on the heating value of a producer gas from gasification of various types of biomass. Increased accuracy of prediction of C_xH_y concentration, thanks to the introduction of the reactions responsible for the generation of propane during gasification, allowed better prediction of heating value. This is essential for the assessment of the performance of BECSS installations based on gasification of sewage sludge since the release of chemical energy during combustion in oxygen is crucial in terms of combustors' temperatures, thus having a high impact on the technical feasibility of particular designs. Further research on plasma gasification is recommended for future validation of the model at high gasification temperatures, which could be achieved, e.g. in plasma gasification.

CRediT author statement

Paweł Ziółkowski Conceptualization, methodology, software, validation; formal analysis, investigation, resources, data curation, writing—original draft preparation, writing—review and editing, visualization, supervision, project administration, funding acquisition. Janusz Badur Conceptualization, supervision, writing—original draft preparation, project administration. Halina Pawlak- Kruczek Conceptualization, supervision, writing—original draft preparation, project administration, funding acquisition. Kamil Stasiak Conceptualization, methodology, software, validation; formal analysis, investigation, resources, data curation, writing—original draft preparation, writing—review and editing, visualization. Milad Amiri formal analysis. Lukasz Niedzwiecki Conceptualization, methodology, software, validation; formal analysis, investigation, resources, data curation, writing—original draft preparation, writing—review and editing. Krystian Krochmalny methodology, formal analysis, investigation. Jakub Mularski validation; formal analysis, investigation, data curation, writing—review and editing. Paweł Madejski funding acquisition. Dariusz Mikielewicz Conceptualization, supervision,-writing—original draft preparation, project administration, funding acquisition. All authors have read and agreed to the published version of the manuscript.

Declaration of competing interest

The authors declare that they have no known competing financial interests or personal relationships that could have appeared to influence the work reported in this paper.

Acknowledgements

The research leading to these results has received funding from the Norway Grants 2014–2021 via the National Center for Research and Development.

Article has been prepared within the frame of the project: "Negative CO_2 emission gas power plant" - NOR/POLNORCCS/NEGATIVE–CO_2–PP/0009/2019–00 which is co-financed by programme "Applied research" under the Norwegian Financial Mechanisms 2014–2021 POLNOR CCS 2019 - Development of CO_2 capture solutions integrated in power and industry processes.

References

[1] United Nations. The Paris agreement | UNFCCC. United nations framew conv clim chang. 2016. https://unfccc.int/process-and-meetings/the-paris-agreement/the-paris-agreement. [Accessed 4 February 2021].

[2] Masson-Delmotte V, Zhai P, Pörtner H-O, Roberts D, Skea J, Shukla PR, et al. Global Warming of 1.5°C. An IPCC Special Report on the impacts of global warming of 1.5°C above pre-industrial levels and related global greenhouse

gas emission pathways, in the context of strengthening the global response to the threat of climate change. 2019.
[3] Hansen K, Breyer C, Lund H. Status and perspectives on 100% renewable energy systems. Energy 2019;175:471–80. https://doi.org/10.1016/j.energy.2019.03.092.
[4] Tzelepi V, Zeneli M, Kourkoumpas DS, Karampinis E, Gypakis A, Nikolopoulos N, et al. Biomass availability in europe as an alternative fuel for full conversion of lignite power plants: a critical review. Energies 2020;13. https://doi.org/10.3390/en13133390.
[5] Roman K, Barwicki J, Rzodkiewicz W, Dawidowski M. Evaluation of mechanical and energetic properties of the forest residues shredded chips during briquetting process. Energies 2021;14:3270. https://doi.org/10.3390/en14113270.
[6] Dudek T. The impacts of the energy potential of forest biomass on the local market: an example of South-Eastern Poland. Energies 2020;13:4985. https://doi.org/10.3390/en13184985.
[7] Niemczyk M, Bachilava M, Wróbel M, Jewiarz M, Kavtaradze G, Goginashvili N. Productivity and biomass properties of poplar clones managed in short-rotation culture as a potential fuelwood source in Georgia. Energies 2021;14:3016. https://doi.org/10.3390/en14113016.
[8] Jia Y, Wang Y, Zhang Q, Rong H, Liu Y, Xiao B, et al. Gas-carrying enhances the combustion temperature of the biomass particles. Energy 2022;239:121956. https://doi.org/10.1016/j.energy.2021.121956.
[9] Dołzyńska M, Obidziński S, Kowczyk-Sadowy M, Krasowska M. Densification and combustion of cherry stones. Energies 2019;12:1–15. https://doi.org/10.3390/en12163042.
[10] Suardi A, Latterini F, Alfano V, Palmieri N, Bergonzoli S, Karampinis E, et al. Machine performance and HOG fuel quality evaluation in olive tree pruning harvesting conducted using a towed shredder on flat and hilly fields. Energies 2020;13:1–16. https://doi.org/10.3390/en13071713.
[11] Kougioumtzis MA, Kanaveli IP, Karampinis E, Grammelis P, Kakaras E. Combustion of olive tree pruning pellets versus sunflower husk pellets at industrial boiler. Monitoring of emissions and combustion efficiency. Renew Energy 2021;171:516–25. https://doi.org/10.1016/j.renene.2021.02.118.
[12] Fuller A, Maier J, Karampinis E, Kalivodova J, Grammelis P, Kakaras E, et al. Fly ash formation and characteristics from (co-)Combustion of an herbaceous biomass and a Greek lignite (Low-Rank Coal) in a pulverized fuel pilot-scale test facility. Energies 2018;11. https://doi.org/10.3390/en11061581.
[13] Romanowska-Duda Z, Piotrowski K, Wolska B, Debowski M, Zielinski M, Dziugan P, et al. Stimulating effect of ash from sorghum on the growth of lemnaceae—a new source of energy biomass. Springer International Publishing; 2020. p. 341–9. https://doi.org/10.1007/978-3-030-13888-2_34.
[14] Vlachokostas C, Achillas C, Agnantiaris I, Michailidou AV, Pallas C, Feleki E, et al. Decision Support system to implement units of alternative biowaste treatment for producing bioenergy and boosting local bioeconomy. Energies 2020;13:2306. https://doi.org/10.3390/en13092306.
[15] Jackowski M, Niedzwiecki L, Jagiełło K, Uchańska O, Trusek A. Brewer's spent grains — valuable beer industry by-product. Biomolecules 2020;10. https://doi.org/10.3390/biom10121669.
[16] Seruga P, Krzywonos M, Seruga A, Niedzwiecki L, Pawlak-Kruczek H, Urbanowska A. Anaerobic digestion performance: separate collected vs. Mechanical segregated organic fractions of municipal solid waste as feedstock. Energies 2020;13. https://doi.org/10.3390/en13153768.
[17] Wielgosiński G, Czerwińska J, Szufa S. Municipal solid waste mass balance as a tool for calculation of the possibility of implementing the circular economy concept. Energies 2021;14:1811. https://doi.org/10.3390/en14071811.
[18] Werle S, Wilk RK. A review of methods for the thermal utilization of sewage sludge: the Polish perspective. Renew Energy 2010;35:1914–9. https://doi.org/10.1016/j.renene.2010.01.019.
[19] Werle S, Dudziak M. Analysis of organic and inorganic contaminants in dried sewage sludge and by-products of dried sewage sludge gasification. Energies 2014;7:462–76. https://doi.org/10.3390/en7010462.
[20] Kacprzak M, Neczaj E, Fijałkowski K, Grobelak A, Grosser A, Worwag M, et al. Sewage sludge disposal strategies for sustainable development. Environ Res 2017;156:39–46. https://doi.org/10.1016/j.envres.2017.03.010.
[21] Lee LH, Wu TY, Kpy Shak, Lim SL, Ng KY, Nguyen MN, et al. Sustainable approach to biotransform industrial sludge into organic fertilizer via vermicomposting: a mini-review. J Chem Technol Biotechnol 2018;93:925–35. https://doi.org/10.1002/jctb.5490.
[22] Cieślik BM, Namieśnik J, Konieczka P. Review of sewage sludge management: standards, regulations and analytical methods. J Clean Prod 2015;90:1–15. https://doi.org/10.1016/j.jclepro.2014.11.031.
[23] Werle S. Sewage sludge-to-energy management in Eastern europe: a polish perspective. Ecol Chem Eng S 2015;22:459–69. https://doi.org/10.1515/eces-2015-0027.
[24] Pajak T. Thermal Treatment as sustainable sewage sludge management. Environ Protect Eng 2013;39:41–53. https://doi.org/10.5277/EPE130205.
[25] Zubrowska-Sudol M, Walczak J. Effects of mechanical disintegration of activated sludge on the activity of nitrifying and denitrifying bacteria and phosphorus accumulating organisms. Water Res 2014;61:200–9. https://doi.org/10.1016/j.watres.2014.05.029.
[26] Zubrowska-Sudol M, Walczak J. Enhancing combined biological nitrogen and phosphorus removal from wastewater by applying mechanically disintegrated excess sludge. Water Res 2015;76:10–8. https://doi.org/10.1016/J.WATRES.2015.02.041.
[27] Żubrowska-Sudoł M, Podedworna J, Bisak A, Sytek-Szmeichel K, Krawczyk P, Garlicka A. Intensification of anaerobic digestion efficiency with use of mechanical excess sludge disintegration in the context of increased energy production in wastewater treatment plants. E3S Web Conf 2017;22:00208. https://doi.org/10.1051/e3sconf/20172200208.
[28] Wilk M, Magdziarz A, Kalemba I. Characterisation of renewable fuels' torrefaction process with different instrumental techniques. Energy 2015;87:259–69. https://doi.org/10.1016/j.energy.2015.04.073.
[29] Pulka J, Wiśniewski D, Gołaszewski J, Białowiec A. Is the biochar produced from sewage sludge a good quality solid fuel? Arch Environ Protect 2016;42:125–34. https://doi.org/10.1515/aep-2016-0043.
[30] Atienza-Martínez M, Fonts I, ábrego J, Ceamanos J, Gea G. Sewage sludge torrefaction in a fluidized bed reactor. Chem Eng J 2013;222:534–45. https://doi.org/10.1016/j.cej.2013.02.075.
[31] Karki S, Poudel J, Oh S. Thermal pre-treatment of sewage sludge in a lab-scale fluidized bed for enhancing its solid fuel properties. Appl Sci 2018;8:183. https://doi.org/10.3390/app8020183.
[32] Wilk M, Magdziarz A, Jayaraman K, Szymańska-Chargot M, Gökalp I. Hydrothermal carbonization characteristics of sewage sludge and lignocellulosic biomass. A comparative study. Biomass Bioenergy 2019;120:166–75. https://doi.org/10.1016/j.biombioe.2018.11.016.
[33] Aragón-Briceño C, Ross AB, Camargo-Valero MA. Evaluation and comparison of product yields and bio-methane potential in sewage digestate following hydrothermal treatment. Appl Energy 2017;208:1357–69. https://doi.org/10.1016/j.apenergy.2017.09.019.
[34] Aragón-Briceño CI, Grasham O, Ross AB, Dupont V, Camargo-Valero MA. Hydrothermal carbonization of sewage digestate at wastewater treatment works: influence of solid loading on characteristics of hydrochar, process water and plant energetics. Renew Energy 2020;157:959–73. https://doi.org/10.1016/j.renene.2020.05.021.
[35] Wang S, Persson H, Yang W, Jönsson PG. Pyrolysis study of hydrothermal carbonization-treated digested sewage sludge using a Py-GC/MS and a bench-scale pyrolyzer. Fuel 2020;262:116335. https://doi.org/10.1016/j.fuel.2019.116335.
[36] Romanak K, Fridahl M, Dixon T. Attitudes on carbon capture and storage (CCS) as a mitigation technology within the UNFCCC. Energies 2021;14:629. https://doi.org/10.3390/en14030629.
[37] Hiremath M, Viebahn P, Samadi S. An integrated comparative assessment of coal-based carbon capture and storage (CCS) vis-à-vis renewable energies in India's low carbon electricity transition scenarios. Energies 2021;14:262. https://doi.org/10.3390/en14020262.
[38] Chen L, Sasaki H, Watanabe T, Okajima J, Komiya A, Maruyama S. Production strategy for oceanic methane hydrate extraction and power generation with Carbon Capture and Storage (CCS). Energy 2017;126:256–72. https://doi.org/10.1016/j.energy.2017.03.029.
[39] Cannone SF, Lanzini A, Santarelli M. A review on CO2 capture technologies with focus on CO2-enhanced methane recovery from hydrates. Energies 2021;14:387. https://doi.org/10.3390/en14020387.
[40] Arora A, Kumar A, Bhattacharjee G, Kumar P, Balomajumder C. Effect of different fixed bed media on the performance of sodium dodecyl sulfate for hydrate based CO2 capture. Mater Des 2015;90:1186–91. https://doi.org/10.1016/j.matdes.2015.06.049.
[41] Arora A, Kumar A, Bhattacharjee G, Balomajumder C, Kumar P. Hydrate-based carbon capture process: assessment of various packed bed systems for boosted kinetics of hydrate formation. J Energy Resour Technol 2021:143. https://doi.org/10.1115/1.4048304.
[42] Kotowicz J, Bartela Ł. Optimisation of the connection of membrane CCS installation with a supercritical coal-fired power plant. Energy 2012;38:118–27. https://doi.org/10.1016/j.energy.2011.12.028.
[43] Míguez JL, Porteiro J, Pérez-Orozco R, Gómez MÁ. Technology evolution in membrane-based CCS. Energies 2018;11:1–18. https://doi.org/10.3390/en11113153.
[44] Sieradzka M, Gao N, Quan C, Mlonka-Mędrala A, Magdziarz A. Biomass thermochemical conversion via pyrolysis with integrated CO2 capture. Energies 2020;13. https://doi.org/10.3390/en13051050.
[45] Qvist S, Gładysz P, Bartela Ł, Sowiżdżał A. Retrofit decarbonization of coal power plants—a case study for Poland. Energies 2020;14:120. https://doi.org/10.3390/en14010120.
[46] Gladysz P, Sowizdzal A, Miecznik M, Hacaga M, Pajak L. Techno-economic assessment of a combined heat and power plant integrated with carbon dioxide removal technology: a case study for central Poland. Energies 2020;13. https://doi.org/10.3390/en13112841.
[47] Cloete S, Hirth L. Flexible power and hydrogen production: finding synergy between CCS and variable renewables. Energy 2020;192:116671. https://doi.org/10.1016/j.energy.2019.116671.
[48] Gładysz P, Stanek W, Czarnowska L, Węcel G, Ø Langørgen. Thermodynamic assessment of an integrated MILD oxyfuel combustion power plant. Energy 2017;137:761–74. https://doi.org/10.1016/j.energy.2017.05.117.
[49] Gładysz P, Stanek W, Czarnowska L, Sładek S, Szlęk A. Thermo-ecological evaluation of an integrated MILD oxy-fuel combustion power plant with CO2 capture, utilisation, and storage – a case study in Poland. Energy 2018;144:379–92. https://doi.org/10.1016/j.energy.2017.11.133.
[50] Ziółkowski P, Badur J. A study of a compact high-efficiency zero-emission power plant with oxy-fuel combustion. In: Stanek W, Gładysz P, Werle S, Adamczyk W, editors. Proc. 32nd int. Conf. Effic. Cost, optim. Simul. Environ.

Impact energy syst., wrocław; 2019. p. 1567–78.
[51] Ziółkowski P, Kowalczyk T, Lemański M, Badur J. On energy, exergy, and environmental aspects of a combined gas-steam cycle for heat and power generation undergoing a process of retrofitting by steam injection. Energy Convers Manag 2019;192:374–84. https://doi.org/10.1016/j.enconman.2019.04.033.
[52] Ziółkowski P, Madejski P, Amiri M, Kuś T, Stasiak K, Subramanian N, et al. Thermodynamic analysis of negative CO2 emission power plant using Aspen Plus, Aspen Hysys, and Ebsilon software. Energies 2021;14:6304. https://doi.org/10.3390/en14196304.
[53] Ramachandran S, Yao Z, You S, Massier T, Stimming U, Wang CH. Life cycle assessment of a sewage sludge and woody biomass co-gasification system. Energy 2017;137:369–76. https://doi.org/10.1016/j.energy.2017.04.139.
[54] Fang S, Deng Z, Lin Y, Huang Z, Ding L, Deng L, et al. Investigation of the nitrogen migration characteristics in sewage sludge during chemical looping gasification. Energy 2021;216:119247. https://doi.org/10.1016/j.energy.2020.119247.
[55] Luo H, Lu Z, Jensen PA, Glarborg P, Lin W, Dam-Johansen K, et al. Effect of gasification reactions on biomass char conversion under pulverized fuel combustion conditions. Proc Combust Inst 2020. https://doi.org/10.1016/j.proci.2020.06.085.
[56] Sirirermrux N, Laohalidanond K, Kerdsuwan S. Kinetics of gaseous species formation during steam gasification of municipal solid waste in a fixed bed reactor. J Energy Resour Technol 2019;1. https://doi.org/10.1115/1.4044193.
[57] Werle S. Sewage sludge gasification: theoretical and experimental investigation. Environ Protect Eng 2013;39:25–32. https://doi.org/10.5277/EPE130203.
[58] Werle S. Impact of feedstock properties and operating conditions on sewage sludge gasification in a fixed bed gasifier. Waste Manag Res 2014;32:954–60. https://doi.org/10.1177/0734242X14535654.
[59] Werle S, Dudziak M. Evaluation of the possibility of the sewage sludge gasification gas use as a fuel. Ecol Chem Eng S 2016;23:229–36. https://doi.org/10.1515/eces-2016-0015.
[60] Szwaja S, Kovacs VB, Bereczky A, Penninger A. Sewage sludge producer gas enriched with methane as a fuel to a spark ignited engine. Fuel Process Technol 2013;110:160–6. https://doi.org/10.1016/j.fuproc.2012.12.008.
[61] Werle S. Numerical analysis of the combustible properties of sewage sludge gasification gas. Chem Eng Trans 2015:1021–6. https://doi.org/10.3303/CET1545171.
[62] Schweitzer D, Gredinger A, Schmid M, Waizmann G, Beirow M, Spörl R, et al. Steam gasification of wood pellets, sewage sludge and manure: gasification performance and concentration of impurities. Biomass Bioenergy 2018;111:308–19. https://doi.org/10.1016/j.biombioe.2017.02.002.
[63] Akkache S, Hernández AB, Teixeira G, Gelix F, Roche N, Ferrasse JH. Co-gasification of wastewater sludge and different feedstock: feasibility study. Biomass Bioenergy 2016;89:201–9. https://doi.org/10.1016/j.biombioe.2016.03.003.
[64] Jamróz P, Kordylewski W, Wnukowski M. Microwave plasma application in decomposition and steam reforming of model tar compounds. Fuel Process Technol 2018;169:1–14. https://doi.org/10.1016/j.fuproc.2017.09.009.
[65] Striūgas N, Valinčius V, Pedišius N, Poškas R, Zakarauskas K. Investigation of sewage sludge treatment using air plasma assisted gasification. Waste Manag 2017;64:149–60. https://doi.org/10.1016/j.wasman.2017.03.024.
[66] McDade JE. Legionella and the prevention of legionellosis. Emerg Infect Dis 2008;14:1006a–1006. https://doi.org/10.3201/eid1406.080345.
[67] Yin Z, Hoffmann M, Jiang S. Sludge disinfection using electrical thermal treatment: the role of ohmic heating. Sci Total Environ 2018;615:262–71. https://doi.org/10.1016/j.scitotenv.2017.09.175.
[68] Sikarwar VS, Zhao M, Clough P, Yao J, Zhong X, Memon MZ, et al. An overview of advances in biomass gasification. Energy Environ Sci 2016;9:2939–77. https://doi.org/10.1039/c6ee00935b.
[69] Ferreira S, Monteiro E, Brito P, Vilarinho C. A holistic review on biomass gasification modified equilibrium models. Energies 2019;12:1–31. https://doi.org/10.3390/en12010160.
[70] Basu P. Biomass gasification, pyrolysis and torrefaction: practical design and theory. Elsevier; 2013. https://doi.org/10.1016/C2011-0-07564-6.
[71] Ferreira S, Monteiro E, Brito P, Vilarinho C. A holistic review on biomass gasification modified equilibrium models. Energies 2019;12:160. https://doi.org/10.3390/en12010160.
[72] Gambarotta A, Morini M, Zubani A. A non-stoichiometric equilibrium model for the simulation of the biomass gasification process. Appl Energy 2018;227:119–27. https://doi.org/10.1016/j.apenergy.2017.07.135.
[73] Żogała A. Equilibrium simulations of coal gasification – factors affecting syngas composition. J Sustain Min 2014;13:30–8. https://doi.org/10.7424/jsm140205.
[74] Costa M, La Villetta M, Massarotti N. Optimal tuning of a thermo-chemical equilibrium model for downdraft biomass gasifiers. Chem Eng Trans 2015;43:439–44. https://doi.org/10.3303/CET1543074.
[75] Cempa-Balewicz M, Jacek Łączny M, Smoliński A, Iwaszenko S. Equilibrium model of steam gasification of coal. J Sustain Min 2013;12:21–8. https://doi.org/10.7424/jsm130203.
[76] de Andrés JM, Vedrenne M, Brambilla M, Rodríguez E. Modeling and model performance evaluation of sewage sludge gasification in fluidized-bed gasifiers using Aspen Plus. J Air Waste Manag Assoc 2019;69:23–33. https://doi.org/10.1080/10962247.2018.1500404.
[77] Król D, Poskrobko S. High-methane gasification of fuels from waste - experimental identification. Energy 2016;116:592–600.
[78] Kozaczka J. Procesy zgazowania : inżynierskie metody obliczeń (in Polish). Kraków: Wydaw. AGH; 1994.
[79] Sharma AK. Equilibrium and kinetic modeling of char reduction reactions in a downdraft biomass gasifier: a comparison. Sol Energy 2008;82:918–28. https://doi.org/10.1016/j.solener.2008.03.004.
[80] Jaworski TJ. Ocena metod obliczania parametrów zgazowania odpadów oraz ich eksperymentalna weryfikacja. Przem Chem 2015;94:1388–91. https://doi.org/10.15199/62.2015.8.28.
[81] Pala LPR, Wang Q, Kolb G, Hessel V. Steam gasification of biomass with subsequent syngas adjustment using shift reaction for syngas production: an Aspen Plus model. Renew Energy 2017;101:484–92. https://doi.org/10.1016/j.renene.2016.08.069.
[82] Kantorek M, Jesionek K, Polesek-Karczewska S, Ziółkowski P, Badur J. Thermal utilization of meat and bone meals. Performance analysis in terms of drying process, pyrolysis and kinetics of volatiles combustion. Fuel 2019;254. https://doi.org/10.1016/j.fuel.2019.05.131.
[83] Elmaz F, Yücel Ö, Mutlu AY. Predictive modeling of biomass gasification with machine learning-based regression methods. Energy 2020;191:116541. https://doi.org/10.1016/j.energy.2019.116541.
[84] Gómez-Barea A, Leckner B. Modeling of biomass gasification in fluidized bed. Prog Energy Combust Sci 2010;36:444–509. https://doi.org/10.1016/j.pecs.2009.12.002.
[85] Topolski J. PhD dissertation: "Diagnostyka spalania w układach gazowo - parowych." (in Polish) - supervisor prof. Janusz Badur. IMP PAN Gdańsk (eng. IFFM PAS); 2002.
[86] Ziółkowski P, Kantorek M. Experiments and numerical modeling of meat and bone meal pyrolysis in a rotary kiln. PhD Interdisciplinary Journal, GTU 2012;1:34–40.
[87] Gumz W. Vergasung fester brennstoffe. 1952. https://doi.org/10.1007/978-3-662-13369-9.
[88] Arlabosse P, Chavez S, Prevot C. Drying of municipal sewage sludge: from a laboratory scale batch indirect dryer to the paddle dryer. Braz J Chem Eng 2005;22:227–32. https://doi.org/10.1590/S0104-66322005000200009.
[89] Sepe AM, Li J, Paul MC. Assessing biomass steam gasification technologies using a multi-purpose model. Energy Convers Manag 2016;129:216–26. https://doi.org/10.1016/j.enconman.2016.10.018.
[90] Lee U, Chung JN, Ingley HA. High-temperature steam gasification of municipal solid waste, rubber, plastic and wood. Energy Fuels 2014;28:4573–87. https://doi.org/10.1021/ef500713j.
[91] Nipattummakul N, Ahmed I, Kerdsuwan S, Gupta AK. High temperature steam gasification of wastewater sludge. Appl Energy 2010;87:3729–34. https://doi.org/10.1016/j.apenergy.2010.07.001.
[92] Mohd Jakarni F, Ni Md Yusoff, Wu J, A Aziz MM. Utilization of sewage sludge molten slag as aggregate substitute in asphalt mixtures. J Teknol 2015;73:105–10. https://doi.org/10.11113/jt.v73.4302.
[93] Mączka T, Śliwka E, Wnukowski M. Plasma gasification of waste plastics. J Ecol Eng 2013;14:33–9. https://doi.org/10.5604/2081139X.1031534.
[94] Diaz G, Sharma N, Leal-Quiros E, Munoz-Hernandez A. Enhanced hydrogen production using steam plasma processing of biomass: experimental apparatus and procedure. Int J Hydrogen Energy 2015;40:2091–8. https://doi.org/10.1016/j.ijhydene.2014.12.049.